

Assessment of the Possibility of the Laser Welding of High Strength Steel Having a Yield Point of 1100 MPa

Abstract: The article presents selected results of technological tests involving the welding of high-strength steel (with a guaranteed yield point of 1100 MPa) using a robotic laser beam welding station. The joints made in the tests were subjected to visual, macroscopic and microscopic tests as well as to hardness measurements. The obtained results revealed the presence of martensitic-bainitic structure in the cross section of the welded joint and the presence of a narrow zone characterised by low hardness (softened zone).

Keywords: high-strength (heat-treated) steels, laser welding, robotics

DOI: [10.17729/ebis.2019.6/3](https://doi.org/10.17729/ebis.2019.6/3)

Introduction

Among presently available structural steels, high-strength steels are enjoying growing popularity. The high strength of such steels is obtained in a metallurgical process through a controlled thermo-mechanical treatment. High-strength steels are obtained as a result of the thermomechanical treatment or toughening. High-strength steels according to PN-EN 10025-6 include a group of steels having a guaranteed yield point of up to 960 MPa. In turn, the product range offered by SSAB or TyssenKrupp includes steels characterised by even higher strength, e.g. S1100 or S1300. However, an increase in the yield point comes at the expense of the reduced weldability of these steels [1]. An increase in the yield point is connected with the obtainment of the appropriate structure, hardness and the chemical composition of steel. As a result, if the content of carbon and the carbon equivalent are relatively low,

a decrease in toughness or the effect of softening in the heat affected zone may be of key importance as regards the functional properties of welded joints. An important aspect related to the welding of high-strength steels is a relatively low heat input to the steel. Because of this, arc welding processes should be automated and, in many cases, replaced with welding processes characterised by high power density such as laser beam welding, electron beam welding or hybrid processes. The application of the above-named processes enables the reduction of the negative effect of the welding thermal cycle on mechanical properties.

Steels subjected to toughening are characterised by hard, i.e. martensitic or martensitic-bainitic, structure. The above-named fact limits machinability during the pre-weld preparation of edges. Another negative aspect is the adverse effect of heat as an excessive heat

input to steel results in its tempering. In addition, in steels containing a molybdenum addition, the heating of the metal to a temperature below that of tempering may trigger the precipitation of molybdenum carbides, located along grain boundaries and responsible for the brittleness (low toughness) of welded joints. A heat input can take place during welding or as a result of heat-related processes (application of excessively high temperature) during operation. The above-presented situation may lead to a significant decrease in mechanical properties (as a result and, consequently, the deterioration of the functional properties of a product). The foregoing leads to the conclusion that the appropriate control of a heat input to the material is crucial for the welding process [2].

The article presents selected test results related to the welding of toughened steel having a yield point of 1100 MPa made using a robotic laser beam welding station. The test results include the results of microstructural tests and those of Vickers hardness tests.

Laser beam welding station

To provide required welding process efficiency, the robotic welding station was equipped with a laser beam-based welding power source IPG Photonics having a power of 6 kW, an M710iC robot (Fanuc) and a biaxial welding positioner. Welding parameters were controlled using the robot control system. Figure 1 presents the schematic diagram of the welding station, whereas Figure 2 presents an exemplary welding cell. The crucial aspect of a laser welding cell is the application of a tight screen separating the cell interior from its surroundings and aimed to prevent health and life hazards resulting from laser radiation.

The use of the welding robot arm as the manipulator of the welding arm enabled fast, precise and repeatable movements of the laser head along edges being joined. The welding tests revealed that it was possible to make precise butt welded joints of 6 mm thick plates.

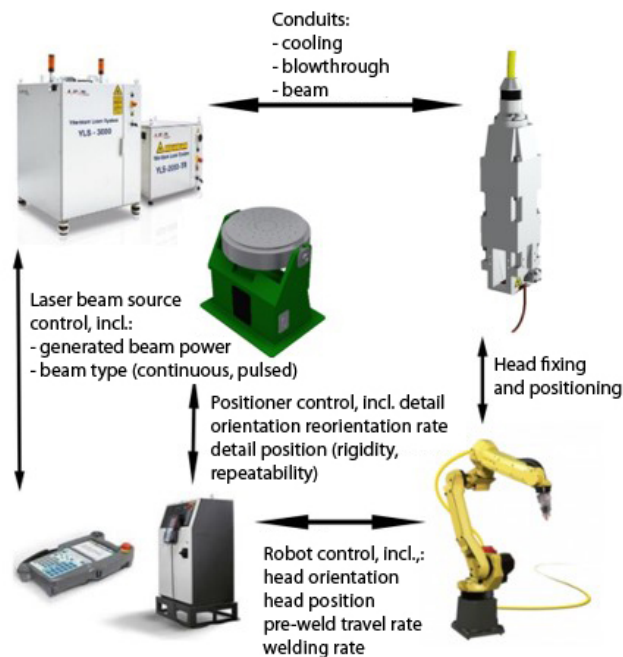


Fig. 1. Schematic integration of the components of the robotic laser beam welding station

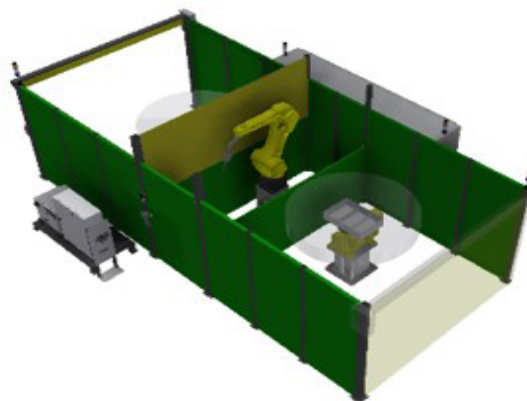


Fig. 2. Exemplary welding cell for laser beam welding processes – model in the RoboGuide environment; two-sided station with a screen and a 2-axial positioner

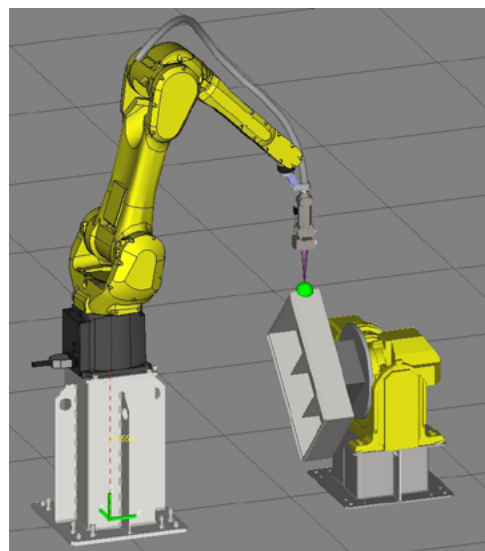


Fig. 3. Exemplary modelling of the technological welding process for a laser beam welding station equipped with a welding robot integrated with a 2-axial positioner; a workpiece (housing) is fixed to the positioner

The application of the computer-aided systems (where all welding station elements are defined) for the modelling of technological processes enabled the fast design of the welding trajectory as well as made it possible to verify if the fixtures were used properly (already at the design stage and not during welding tests).

Test material

The tests involved the use of 6 mm thick plates made of steel having a yield point of 1100 MPa. The chemical composition and selected mechanical properties of the steel are presented in Table 1. The plates (100 mm × 250 mm) were cut out using the abrasive blasting process. Afterwards, the plates were subjected to cleaning performed to remove residual corrosion and other impurities. The process of welding was performed along the longer edge. Before welding, the edges were subjected to grinding. The gap between the ground surfaces mounted to less than 0.1 mm. The plates were joined by means of terminally located tack welds. The welding process was performed at a rate restricted within the range of 1 m/min to 3 m/min and beam power restricted within the range of 4 kW to 6 kW. The most favourable geometry of the face and root was obtained using a welding rate of 1.5 m/min and a power of 5 kW. The welding process enabled the obtainment of a butt joint with full penetration in one run of the beam.

Table 1. Chemical composition and selected mechanical properties of steel S1100QL according to ThyssenKrupp, heat analysis, % by weight

C	Si	Mn	Cr	Ni	Mo	V
≤0.2	≤0.50	≤1.70	≤1.70	≤2.50	≤0.70	≤0.012
S – max. 0.005		P – max. 0.02		B – max. 0.005		
Yield point, R_{eH} (MPa)		Tensile strength, R_m (MPa)		Elongation A (%)		
1100		1200–1500		8		

Visual assessment and macroscopic tests

The visual assessment of the welded joint was based on the PN-EN ISO 17637 standard.

The joint represented quality level B according to PN-EN ISO 13919-1. Figure 4a presents a fragment of the weld face after welding with visible layers of tarnish.

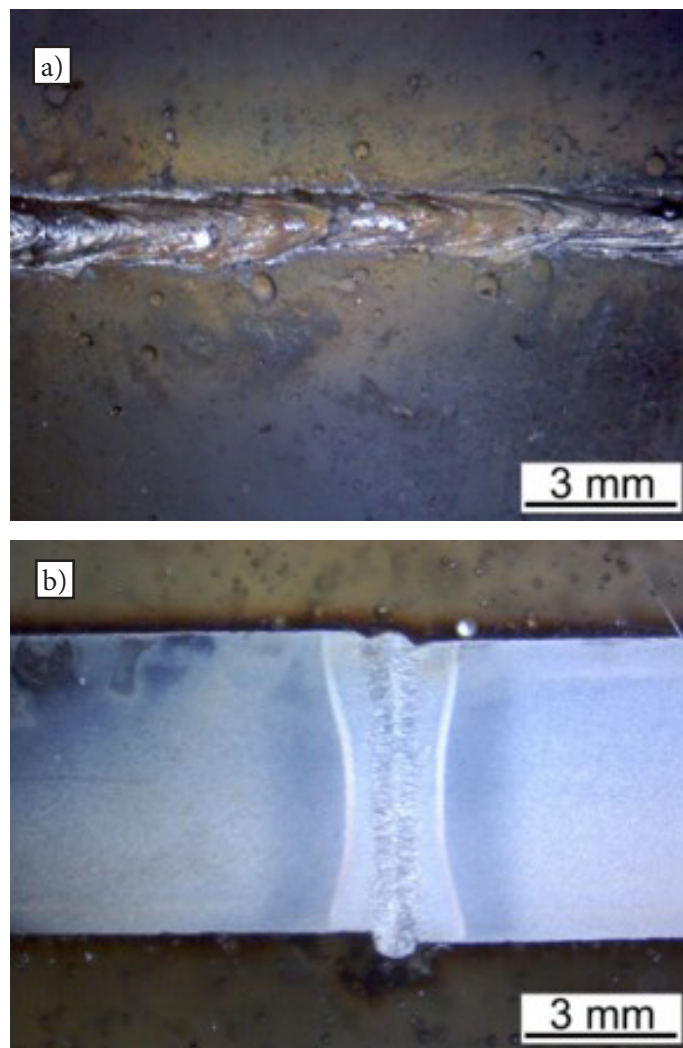


Fig. 4. Weld face (a) and the macrostructure in the cross-section of the joint (b)

To reveal the macrostructure of the welded joint it was necessary to sample the latter in the cross-section perpendicular to the weld axis. The specimen was included in epoxy resin and subjected to grinding with water-based abrasive paper and polishing with polishing cloth and the water slurry of Al_2O_3 . The metallographic specimen prepared as described above was subjected to chemical etching in the 4% alcohol solution of nitric acid. The test revealed the regular shape of the face and that of the root. On the root side it was possible to notice slight excessive penetration whereas on the face side it was possible to observe slight two-sided concavity (below 0.1 mm). In addition, it was possible to notice the slight

misalignment of the joined edges. The obtained weld was characterised by a symmetric shape and a uniform width restricted within the range of approximately 0.8 mm to 0.9 mm, which corresponded to a joint shape factor of (b/h) restricted within the range of approximately 0.13 to 0.16. The width of the HAZ heated above A_{C1} did not exceed 0.6 mm and was sharply outlined. Within approximately 1.5 mm, it was possible to observe different behaviour during etching. The presence of the concavity of the weld face required the performance of grinding aimed to obtain the surface without the notch, potentially responsible for the reduction of mechanical properties under fatigue and changes of steel properties in the area heated below A_{C1} resulting from the effect of the welding thermal cycle.

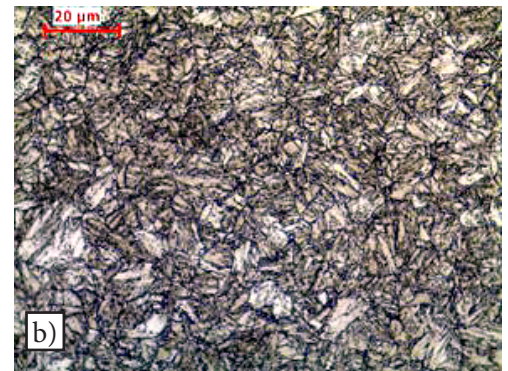
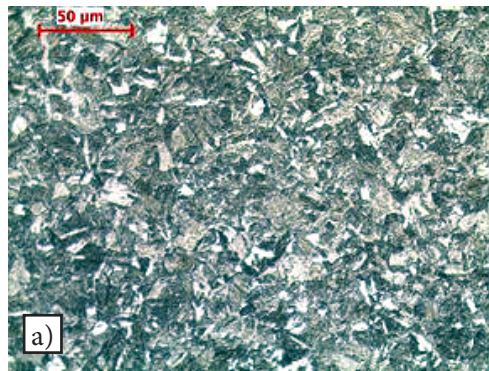
Microscopic tests

The base material was characterised by the fine-grained martensitic structure and martensitic-bainitic structure with dispersive precipitates of carbides and carbonitrides located along boundaries of martensite laths and inside them. The presence of carbides resulted from the presence of molybdenum and vanadium in the chemical composition. A strongly carbide-forming chemical element added to toughened steels is niobium. The presence of carbides enables the formation of the fine-grained structure and the obtainment of favourable mechanical properties. However, the foregoing is also connected with the deterioration of steel weldability because of the tempering effect in the heat affected

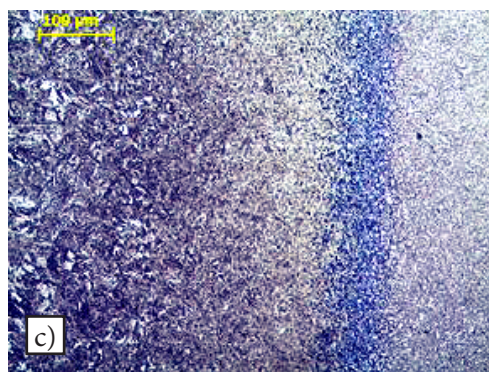
zone and the area adjacent to the HAZ.

The HAZ of the welded joint contained three sharply outlined zones, i.e. a superheated zone, a fine-grained zone and a very narrow zone of partial recrystallization. The above-named areas contained the martensitic or martensitic-bainitic structure (of various morphology). The area heated (during welding) up to a temperature restricted within the range of A_{C1} to A_{C3} (zone of partial recrystallization) contained bright fields of fresh martensite against the dark etching structure of high-tempered martensite. In turn, the superheated area, in the direct vicinity of the fusion line, was characterised by grain growth (very narrow area).

Because of the presence of precipitates of carbides and carbonitrides along the boundaries of former austenite, the 1 mm wide base material area heated below A_{C1} was characterised by sharply outlined boundaries of former austenite grains and the presence of bright areas formed as a result of steel tempering and grain formation

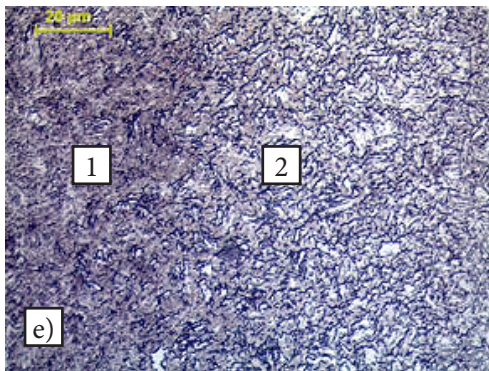


Base material – tempered martensite structure)

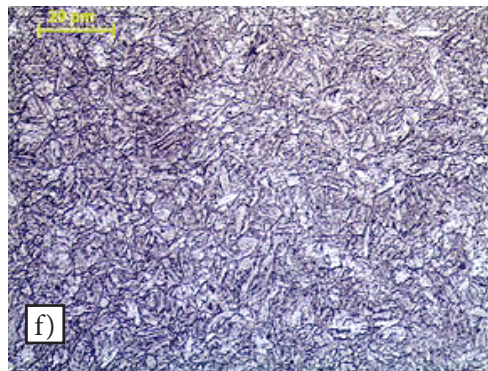


HAZ – microscopic view containing characteristic areas (from the right): superheated zone, fine-grained zone, partial crystallisation zone and base material area

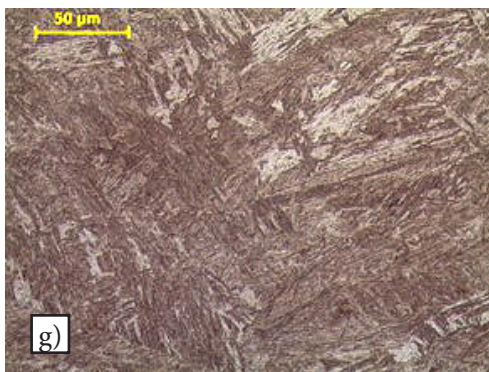
Fine-grained zone (3), partially crystallised zone (2) and base material (1)



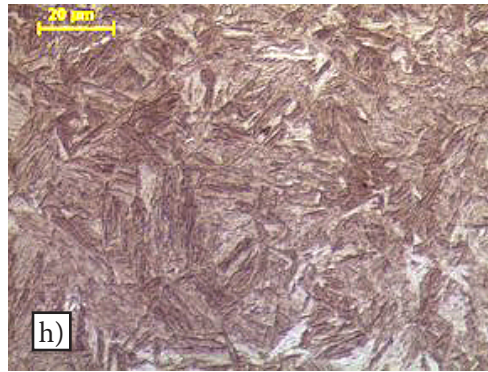
Partially crystallised zone (1) and adjacent area heated below Ac1



Zone of high-tempered martensite heated below Ac1 (visible boundaries of former austenite)



Weld – zone of transcrystallisation in the weld axis; coarse-crystal structure
martensitic structure – lath martensite



load of 3 kG. The tests involved the use of a metallographic specimen perpendicular to the weld axis. The metallographic specimen was subjected to grinding, polishing and chemical etching. Indents were made along the measurement line at the half of the joint depth from the base material side, through the HAZ, weld and the HAZ on the side opposite the base material. The hardness tests revealed that the joint was characterised by a significant scatter of results restricted within the range of approximately 340 HV₃ to 460 HV₃ (i.e. a range of 120 HV₃). In individual areas, changes in hardness

Fig. 5. Microstructure of the welded joint; etchant: 4% Nital (description under the photographs)

The weld contained the martensitic structure with columnar crystals located between the fusion line and the weld axis. The aforesaid arrangement resulted from the narrow width of the weld and the fast discharge of heat to the base material. The arrangement of the columnar crystals, noticed already during the macroscopic tests, was observed along the entire length of the weld (Fig. 4b). Because of the high purity of the steel (low contents of S and P), the crystal contact area did not contain the band of impurities. Exemplary microstructures along with their characteristics are presented in Figure 5.

Hardness measurements

Hardness measurements were based on the Vickers hardness test performed under an indenter

were relatively small in relation to that of the base material – approximately 380–400 HV₃ ($R_m=1200-1275$ MPa). The tests revealed an increase in hardness in the weld up to approximately 410–420 HV₃ ($R_m=1330-1385$ MPa) and in the HAZ up to 460 HV₃ ($R_m=1540$ MPa). On the base material side, behind the area of partial

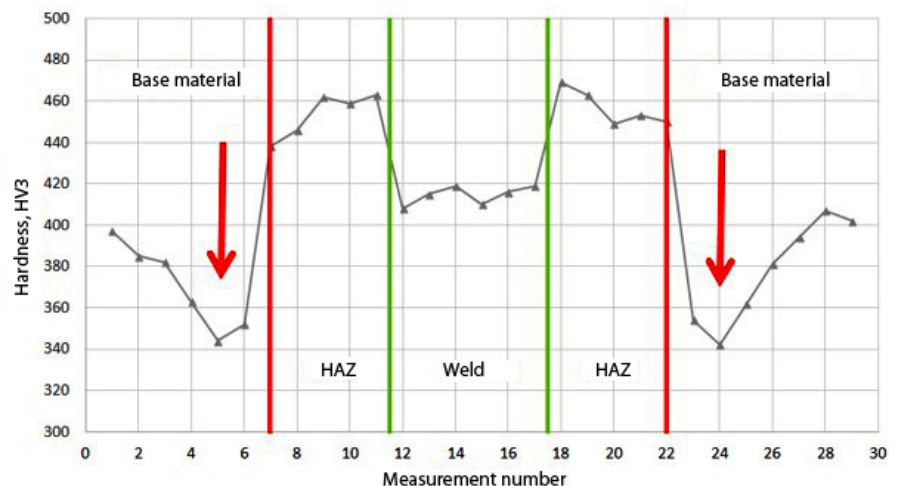


Fig. 6. Distribution of hardness HV₃ in the cross-section of the laser beam welded joint made in steel S1100QL

crystallisation, it was possible to notice a significant decrease in hardness to approximately 340 HV₃ ($R_m=1065$ MPa). The foregoing indicated the presence of the softened zone having a width of approximately 0.6 mm. The hardness decrease in the above-named area in relation to the base material was relatively low, i.e. to approximately 40 HV₃, where the lowest value was obtained only in the area of the first indent (approximately 0.1 mm to 0.2 mm). The presence of such a narrow softened zone did not affect the mechanical properties of the welded joint under axial tension conditions.

Summary

The above-presented tests revealed it is possible to obtain high-quality laser beam filler metal-free welded joints in high-strength steel having a guaranteed yield point of 1100 MPa. However, the welding process should be preceded by the appropriate preparation of edges to be joined in order to obtain the parallelism of the edges and, consequently, a narrow gap (below 0.1 mm) between them. In relation to the 6 mm thick plate, the obtained weld root was slightly convex, whereas the weld face was slightly concave (below 0.1 mm). The revealed weld geometry indicated the necessity of post-weld grinding of the face in structures exposed to fatigue and was responsible for the weld thickness reduction (restricted within the plate tolerance limits).

The weld and HAZ were narrow and symmetric, where individual HAZ areas or the fusion line were nearly parallel. The significant welding rate resulted in a slight increase in hardness in the HAZ, i.e. by approximately 60–70 HV₃ in relation to that of the base material and by approximately 40 HV₃ in comparison with the hardness of the weld. The foregoing indicates that the above-named area will be characterised by lower toughness and lower resistance to fatigue cracking. However, the narrow HAZ area precluded the performance of classical impact strength tests. In the material

heated below A_{cl} it was possible to observe a narrow zone characterised by lower hardness than that of the base material and where tensile strength could be lower (1065 MPa) than the yield point of the base material (above 1100 MPa). Despite the influence of the fast welding thermal cycle, the heat input to the steel triggered the effect of softening, where the width of the softened area decreased along with the reduction of a heat input during welding.

The low contents of admixtures was responsible for the fact that the weld axis did not contain an area of impurities triggering susceptibility to cracking during the welding process. In addition, the hardness decrease in the HAZ (softened zone) was not followed by the deterioration of the mechanical properties of the welded joint (immediate strength). However, the foregoing may affect fatigue strength. The welded joint contained the martensitic structure composed of lath martensite.

Acknowledgements

The welding tests were performed using a robotic laser beam welding station built by Roboty Przemysłowe Sp. z o.o. within project *The Development and Implementation of an Innovative High-Performance Technology for the Joining of High-Strength Steel Having a Yield Point of 1300 MPa Using the Laser Beam and a Robotic Welding Station POIR.01.01.01-00-1072/15*.

The tests of the welded joints were performed within research work 16.16.110.663 (task 5).

References

- [1] Tasak E.: Metalurgia spawania. Wydawnictwo JAK, Kraków, 2008
- [2] Tasak E., Ziewiec A.: Spawalność materiałów konstrukcyjnych. Tom 1. Spawalność stali. Wydawnictwo JAK, Kraków, 2009.

Related standards

- PN-EN ISO 17637 Badania nieniszczące złączy spawanych – Badania wizualne złączy spawanych

- PN-EN ISO 13919-1 Spawanie – Złącza spawane wiązką elektronów i wiązką promieniowania laserowego – Wytyczne do określania poziomów jakości według niezgodności spawalniczych – Część 1: Stal.
- PN-EN 10025-6 Wyroby walcowane na gorąco ze stali konstrukcyjnych – Część 6: Warunki techniczne dostawy wyrobów płaskich o podwyższonej granicy plastyczności w stanie ulepszonym cieplnie.